MONOCLONAL ANTIBODIES IN IMMUNODIAGNOSIS AND IMMUNOTHERAPY
Volume 41, Number 4, 2022
Mary Ann Liebert, Inc.
DOI: 10.1089/mab.2021.0068

Short Communications

Open camera or QR reader and scan code to access this article and other resources online.

A Comparison of Murine PD-1 and PD-L1 Monoclonal Antibodies

Melissa T. Bu,[1,2] Long Yuan,[1,2] Alyssa N. Klee,[1,2] and Gordon J. Freeman[1,2]

Blockade of the PD-L1/PD-1 pathway has proven to be a broadly effective cancer immunotherapy. FDA-approved therapeutic monoclonal antibodies (mAbs) targeting the pathway have high affinity, blocking capacity, and low antibody effector activity. A number of rat antimouse mAbs have been used to model cancer immunotherapy in mouse models. We set forth the amino acid sequences of mAbs specific for mouse PD-1 (29F.1A12) and PD-L1 (10F.9G2) and compare their avidities, blocking capacities, biological activities, and epitope recognition with other commonly used mAbs. Further manipulation of these sequences should facilitate better modeling of immunotherapy in mouse models and the generation of novel agents.

Keywords: PD-1, PD-L1, cancer immunotherapy, monoclonal antibody, antibody sequences

Introduction

PD-1 is an inhibitory receptor expressed on the cell surface of activated T cells.[1] Its ligands, PD-L1 and PD-L2, can be expressed on antigen presenting cell surfaces and engage an immunoinhibitory signal through PD-1. In addition, PD-L1 is often—and PD-L2 less frequently—expressed on tumor cells and can mediate immune evasion of tumors.[2–5] PD-L1 can also be widely expressed on nonhematopoietic cells (e.g., epithelial cells, vascular and lymphatic endothelial cells, keratinocytes, mesenchymal stem cells, and placental syncytiotrophoblasts) as well as hematopoietic cells (e.g., dendritic cells, macrophages, T cells, NK cells, B cells, and mast cells). PD-L2 expression is more restricted to hematopoietic cells.

Blockade of the interaction of PD-1 with its ligands enhances T cell activation, cytokine production, and cytolysis, and has been translated into effective cancer immunotherapies. The antimurine PD-L1 monoclonal antibodies (mAbs), 9G2 and MIH6, were first reported in 2002.[6,7] Numerous antimurine PD-1 mAbs have also been reported including 1A12, RMP1-14, and RMP1-30.[8–10] PD-1 and PD-L1 mAbs have demonstrated efficacy in many murine tumor immunotherapy models.[11,12] Seven antihuman PD-1 and PD-L1 mAbs have been FDA approved as cancer immunotherapies and have displayed unprecedented clinical efficacy.[11–13]

Nevertheless, numerous questions regarding the PD-1/PD-L1 pathway and optimal combination therapies remain unanswered and better experimental modeling would strengthen the clinical relevance of preclinical investigations. In this study, we report the variable region sequences of the PD-1 mAb, 1A12, and PD-L1 mAb, 9G2. These sequences should facilitate the design of novel engineered forms of the mAbs for PD-1 pathway investigation.

Materials and Methods

Antibodies and fusion proteins

PD-L1 mAb (9G2, rat IgG2b) was purchased from BioXcell (Lebanon, NH).[6,14] Unconjugated and fluorophore-conjugated PD-1 mAbs (1A12, rat IgG2a; RMP1-14, rat IgG2a; and RMP1-30, rat IgG2b) and PD-L1 mAbs (10F.9G2, rat IgG2b; MIH6, rat IgG2a) were purchased from BioLegend (San Diego, CA).[8–10,15] Similar PD-1 mAb staining and blocking results were seen using unconjugated PD-1 mAbs purchased from BioXcell (Supplementary

[1]Department of Medical Oncology, Dana-Farber Cancer Institute, Boston, Massachusetts, USA.
[2]Department of Medicine, Harvard Medical School, Boston, Massachusetts, USA.

Figs. S1 and S2). Isotype control mAbs were purchased from BioXcell. Mouse (m) PD-L1, PD-L2, CD80, and PD-1 human IgG1 Fc fusion proteins were purchased from R&D (Minneapolis, MN). 10F.5C5 (rat IgG2b) was made as described.[9]

Cell lines and cell culture

300.19 cells are an Abelson leukemia virus transformed pre-B cell line. 300-mPD-1 and 300-mPD-L1 transfected cell lines were previously established in the laboratory[16] through transfection of cDNA constructs in an antibiotic resistance vector through electroporation and selection in medium containing the selective agent. 300-mPD-1 and 300-mPD-L1 were maintained in R10 medium, which consists of RPMI-1640 medium (Life Technologies, Carlsbad, CA), 10% fetal bovine serum (FBS; Life Technologies), 1% Gluta-Max (Life Technologies), 1% penicillin–streptomycin (HyClone, Logan, UT), and 15 μg/mL gentamicin (Life Technologies), supplemented with 0.05 mM beta-mercaptoethanol and 5 μg/mL puromycin (InvivoGen, San Diego, CA).

Jurkat T cell lymphoma (TIB-152) cell line was obtained from the ATCC (Manassas, VA). Jurkat cells expressing mouse PD-1 (mPD-1-Jurkat) were previously established in the laboratory. mPD-1-Jurkat cells were maintained in R10 medium supplemented with 1 μg/mL puromycin. Mouse PD-L1/T-cell receptor (TCR) activator (anti-CD3 scFv)-CHO cells (BPS Bioscience, San Diego, CA) were maintained in F12-K medium (Life Technologies) containing 10% FBS, 1% Gluta-Max, and 1% penicillin–streptomycin (HyClone), with 750 μg/mL G418 (Life Technologies), and 500 μg/mL hygromycin (Invitrogen, Carlsbad, CA).

TCR activator (anti-CD3 scFv)-CHO cells (BPS Bioscience) were maintained in F12-K medium containing 10% FBS, 1% Gluta-Max, 1% penicillin–streptomycin, with 500 μg/mL hygromycin. Mouse PD-1/nuclear factor of activated T-cells (NFAT) reporter-Jurkat cells (BPS Bioscience) were maintained in RPMI-1640 medium containing 10% FBS, 1% Gluta-Max, 1% penicillin/streptomycin, 10 mM hydroxyethyl piperazineethanesulfonic acid (HEPES) (Life Technologies), 1 mM sodium pyruvate (Life Technologies), with 500 μg/mL of G418, and 0.25 μg/mL puromycin. All cells were kept at 37°C with 5% CO_2. ATCC-derived cell lines were cultured no more than 3 months before a new thaw was initiated. All Jurkat and 300.19 parental cell lines and stable transfected cell lines were tested for mycoplasma and the results were negative using the Venor GeM Mycoplasma Detection Kit (Sigma-Aldrich, St. Louis, MO).

PD-1 and PD-L1 specificity assay

PD-1 and PD-L1 mAbs were diluted in flow cytometry buffer (phosphate-buffered saline, 2% FBS, 0.02% sodium azide) twofold 12 times beginning at 10 μg/mL. The indicated concentrations of PD-1 or PD-L1 mAbs were incubated with mPD-1–transfected Jurkat cells or mPD-L1–transfected 300.19 cells, respectively, for 30 minutes at 4°C. Cells were washed twice, and binding was detected using 10 μg/mL phycoerythrin (PE)-conjugated goat antirat-IgG (Southern Biotech, Birmingham, AL). Cells were washed and analyzed by flow cytometry. EC_{50} and IC_{50} analyses were conducted using GraphPad Prism.

PD-L1 binding to PD-1 blocking assay

The indicated concentrations of PD-1 or PD-L1 mAb were preincubated with mPD-1–transfected Jurkat cells or mPD-L1–transfected 300.19 cells for 30 minutes at 4°C. mPD-L1, mPD-L2, mCD80, or mPD-1 human IgG1 Fc fusion protein was added, and incubation continued for 30 minutes at 4°C. Cells were washed twice, and binding of fusion protein was detected with 5 μg/mL Alexa647-conjugated goat antihuman IgG mAb (multispecies adsorbed; Southern Biotech). Cells were washed and analyzed by flow cytometry.

PD-1 mAb binding to exhausted T cells

Exhausted T cells were prepared as described.[17] $CD8^+$ T cells were purified from C57BL/6-Tg(TcraTcrb)1100Mjb/J (commonly known as OT-I) mouse splenocytes with magnetic beads (Miltenyi Biotec, Auburn, CA). Cells were cultured at a final density of 5×10^5/mL in complete medium (RPMI 1640, 10% FBS, 1% 2 mM L-glutamine, 1% 1 M HEPES, 1% 100 mM sodium pyruvate, 1% nonessential amino acids, 1% penicillin–streptomycin, 0.05 mM beta-mercaptoethanol) with interleukin (IL)-15 (5 ng/mL; Peprotech, East Windsor, NJ) and IL-7 (5 ng/mL; Peprotech) with 10 ng/mL $OVA_{(257–264)}$ peptide (Anaspec, Fremont, CA).

Cells were repetitively stimulated with 10 ng/mL $OVA_{(257–264)}$ peptide daily for 5 to 7 days. Cells were checked daily, and when confluent, split, and cultured with fresh complete medium containing cytokines. For flow cytometry analysis, cells were first incubated with anti-Fc receptor antibody clone 2.4G2 (1 μg per well) for 30 minutes at room temperature. The indicated concentration of PE-conjugated PD-1 mAb 1A12, RMP1-14, or RMP1-30 or isotype control mAb was added and incubated for 30 minutes at 4°C. Cells were washed twice and binding was analyzed by flow cytometry.

PD-1 mAb epitope blocking assay

Jurkat cells stably transfected with mouse PD-1 were incubated with the indicated concentrations of 1A12, RMP1-14, RMP1-30, or isotype control mAbs for 30 minutes at 4°C. PE-conjugated 1A12, RMP1-14, or RMP1-30 mAb was added and incubated for 30 minutes at 4°C. Cells were washed and analyzed by flow cytometry.

PD-L1 mAb epitope blocking assay

300.19 cells stably transfected with mouse PD-L1 were incubated with the indicated concentrations of 10F.9G2, MIH6, 10F.5C5, or isotype control mAbs for 30 minutes at 4°C. PE-conjugated 10F.9G2 or MIH6 mAb was added and incubated for 30 minutes at 4°C. Cells were washed and analyzed by flow cytometry.

Flow cytometry

Cells were examined using a Fortessa X-20 flow cytometer and data were analyzed with FlowJo 10.6. In total, 10,000 to 20,000 cells were analyzed. Data were analyzed with Excel and GraphPad Prism. Graphical, EC_{50}, and IC_{50} analyses were conducted using GraphPad Prism.

T cell activation luciferase reporter assays

Mouse PD-L1-TCR activator-CHO cells and TCR activator-CHO cells were seeded at 3.75×10^4 cells/well in CHOK1 growth medium (F12-K medium containing 10%

FBS; 1% Gluta-Max, and 1% penicillin–streptomycin), in a white 96-well plate (Corning, Corning, NY) and incubated overnight at 37°C with 5% CO_2. The next day, medium was removed, and cells were incubated with the indicated antibodies in 75 μL Jurkat cell medium (RPMI-1640 medium containing 10% FBS, 1% Gluta-Max, 1% penicillin–streptomycin, 10 mM HEPES, 1 mM sodium pyruvate) for 30 minutes before the addition of 50,000 mouse PD-1/NFAT reporter-Jurkat cells/well in 25 μL Jurkat cell medium.

Where added, the final concentration of CD28 antibody (clone 9.3; BioXcell) was 1 μg/mL. After 5 to 6 hours, Luciferase signal was produced by adding 100 μL ONE-Step™ Luciferase Assay System (BPS Bioscience) according to manufacturer's protocol, and luminescence was measured as relative light units (RLU) in a Luminiskan luminometer (Life Sciences, Saint Petersburg, FL). NFAT fold induction was calculated as (Experimental value in RLU − background well without Jurkat in RLU)/(Isotype control without anti-CD28 in RLU − background well without Jurkat in RLU).

Results and Discussion

Owing to the widespread use of both PD-L1 mAbs 9G2 and MIH6 in experimental mouse models, we compared the properties of these two mAbs. The 9G2 and MIH6 antimouse PD-L1 mAbs similarly bound to mPD-L1–transfected 300.19 cells in a dose-dependent manner with an apparent affinity of 0.54 nM (Fig. 1A). In addition, 9G2 and MIH6 were able to block the binding of PD-1-Fc and CD80-Fc to mPD-L1–transfected 300.19 cells in a dose-dependent manner with similar IC_{50} of 0.054 and 0.061 µg/mL (Fig. 1B) and 0.025 and 0.051 µg/mL (Fig. 1C), respectively.

We tested the ability of 9G2 and MIH6 to reverse PD-1–mediated inhibition of a TCR/CD28 signal (Fig. 1D). CHO cells expressing cell surface anti-CD3 scFv and mouse PD-L1 were cocultured with anti-CD28 mAb and Jurkat cells expressing mouse PD-1 and the firefly luciferase gene under the control of NFAT response elements. Luciferase activity was assayed as a measure of T cell activation. Incubation

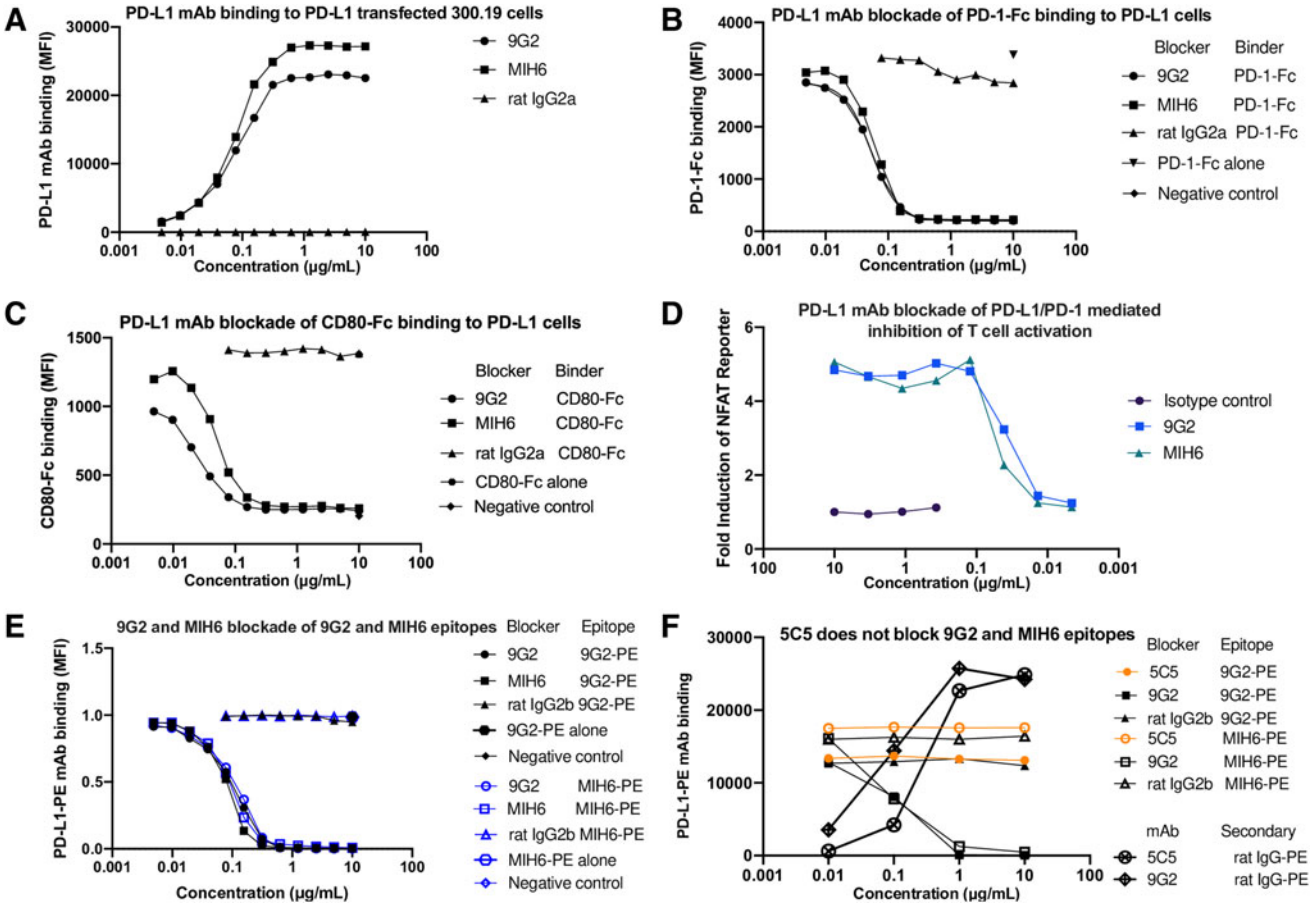

FIG. 1. Staining and blocking capacities of PD-L1 mAbs. Flow cytometric analysis of **(A)** PD-L1 mAbs 9G2 and MIH6 binding to 300.19 cells expressing PD-L1. Replicates $n=4$. **(B)** Capacity of PD-L1 mAbs 9G2 and MIH6 to block binding of PD-1-Fc to 300.19 cells expressing mPD-L1. Replicates $n=3$. **(C)** Capacity of PD-L1 mAbs 9G2 and MIH6 to block binding of CD80-Fc to 300.19 cells expressing mPD-L1. Replicates $n=2$. **(D)** Jurkat NFAT-luciferase reporter T cells expressing mouse PD-1 were cocultured with CHO cells expressing anti-CD3 scFV and mouse PD-L1 with the indicated PD-L1 or isotype control mAbs and 1 µg/mL CD28 mAb. Fold induction of NFAT reporter was calculated as described in Methods section. Replicates $n=2$. **(E)** Flow cytometric analysis of unlabeled 9G2, MIH6, and rat IgG2b blockade of 9G2-PE binding or MIH6-PE binding. Replicates $n=2$. **(F)** Flow cytometric analysis of unlabeled 9G2, 5C5, and rat IgG2b blockade of 9G2-PE binding or MIH6-PE binding. Replicates $n=2$. Separately, PD-L1 mAbs 9G2 and 5C5 binding to 300.19 cells expressing PD-L1. Replicates $n=2$. mAbs, monoclonal antibodies; MFI, median fluorescence intensity; NFAT, nuclear factor of activated T-cells.

with isotype control gave only a low level of luciferase activity, indicating the dominance of the PD-L1/PD-1 inhibitory signal over TCR/CD3 in this system in the absence of any blocking agent. PD-L1 mAbs 9G2 and MIH6 similarly increased luciferase induction in a dose-dependent manner with a maximal induction of fivefold and IC_{50} values of 0.039 and 0.044 μg/mL, respectively.

Epitope blocking studies showed 9G2 and MIH6 cross-blocked themselves and each other equally well (Fig. 1E). These results show that 9G2 and MIH6 are near equivalent mAbs. To identify an mAb that could be used to analyze PD-L1 expression in the presence of 9G2 or MIH6, such as in cells from a cancer immunotherapy experiment, we tested a number of other PD-L1 mAbs and found that 10F.5C5[9] was unable to block binding of 9G2 or MIH6 but had a good affinity ($\sim$3 nM) for PD-L1 (Fig. 1F).

Owing to the widespread use of both PD-1 mAbs 1A12 and RMP1-14 in experimental mouse models, we compared the avidities of these two mAbs. The 1A12 antimouse PD-1 mAb bound to mPD-1–transfected Jurkat cells in a dose-dependent manner with an apparent affinity of 0.42 nM, while RMP1-14 bound with a much weaker apparent affinity of 28.8 nM (Fig. 2A). This result was also seen with 1A12 and RMP1-14 mAbs from a different vendor (BioXcell; Supplementary Fig. S1).

In case the lower avidity of RMP-1-14 was a consequence of transfection, we assayed the antibody binding to exhausted murine CD8 T cells naturally expressing PD-1. Similarly, 1A12 had a higher avidity and maximal fluorescence intensity than RMP1-14 (Fig. 2B). The RMP1-30[10] mouse PD-1 mAb had an intermediate avidity and maximal fluorescence intensity (Fig. 2B).

We tested the ability of 1A12 and RMP1-14 to block the binding of PD-L1 or PD-L2 Fc fusion proteins to mPD-1. Both 1A12 and RMP1-14 blocked the binding of PD-1 to PD-L1 and PD-L2, but consistent with its higher avidity, 1A12 blocked with an IC_{50} of 0.036 and 0.034 μg/mL for PD-L1 and PD-L2, respectively, whereas RMP1-14 blocked with an IC_{50} of 3.23 and 4.05 μg/mL for PD-L1 and PD-L2, respectively (Fig. 2C). These results show that 1A12 and RMP1-14 both block binding to PD-1 ligands but 1A12 is much more effective at lower concentrations because of its higher avidity.

We tested the ability of 9G2, 1A12, RMP1-14, and RMP1-30 to reverse PD-1–mediated inhibition of a TCR/CD28 signal using CHO cells expressing cell surface anti-CD3 scFv and mouse PD-L1 and Jurkat cells expressing mouse PD-1 and the firefly luciferase gene under the control of NFAT response elements (Fig. 2D). PD-L1 mAb 9G2 and PD-1 mAb 1A12 similarly increased luciferase induction in a dose-

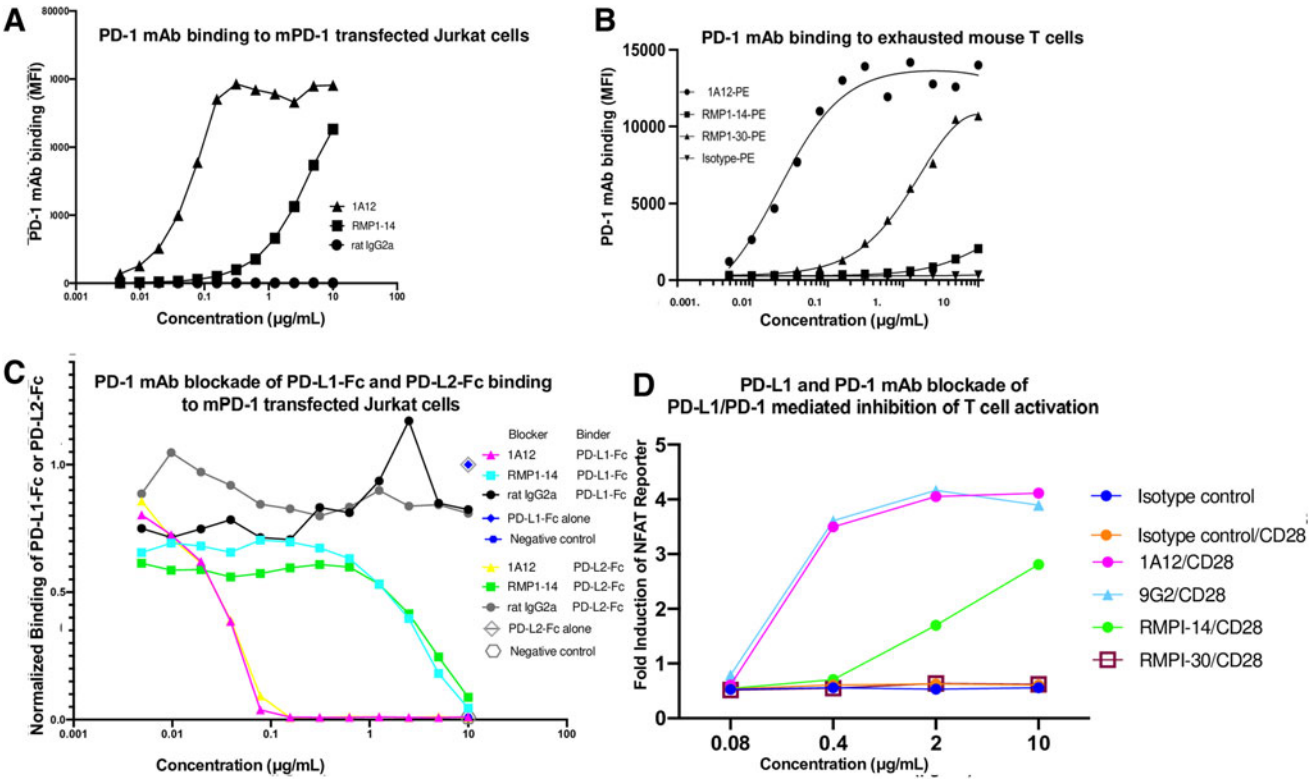

FIG. 2. Staining and blocking capacities of PD-L1 and PD-1 mAbs. Flow cytometric analysis of **(A)** PD-1 mAb 1A12 and RMP1-14 binding to Jurkat cells expressing mPD-1. Replicates $n=5$. **(B)** 1A12-PE, RMP1-14-PE, RMP1-30-PE, and isotype control-PE binding to exhausted mouse T cells. Replicates $n=2$. **(C)** Normalized capacity of 1A12, RMP1-14, or isotype control to block binding of PD-L1-Fc or PD-L2-Fc to Jurkat cells expressing mPD-1. Label indicates blocking agent, followed by binding agent. Replicates $n=2$. **(D)** Jurkat NFAT-luciferase reporter T cells expressing mouse PD-1 were cocultured with CHO cells expressing anti-CD3 scFV and mouse PD-L1 with the indicated PD-1, PD-L1, or isotype control mAbs and 1 μg/mL CD28 mAb. Fold induction of NFAT reporter was calculated as described in Methods section. Replicates $n=2$.

dependent manner with a maximal induction of sevenfold and IC_{50} values of 0.28 μg/mL. PD-1 mAb RMP1-14 increased luciferase induction in a dose-dependent manner with a maximal induction of fivefold and an IC_{50} value of 1.99 μg/mL.

RMP1-30 did not result in any increase in luciferase activity, consistent with its reported inability to block the interaction of PD-L1 with PD-1.[10] In the absence of a PD-1 signal (CHO cells expressing anti-CD3 scFv without PD-L1), the mAbs had no effect on luciferase induction, indicating the antibodies did not transduce a T cell stimulating signal but worked by blocking the PD-1 inhibitory signal (Supplementary Fig. S3). These results indicate that PD-1 and PD-L1 mAbs can reverse the PD-1 inhibitory signal proportionally to the extent they block the binding of PD-L1 to PD-1 (compare Fig. 2C and D).

We also investigated epitope overlap between 1A12, RMP1-14, and RMP1-30 by assaying binding of each PE-conjugated PD-1 mAb to Jurkat-mPD-1 cells in the presence of each unconjugated mAb. 1A12 is able to fully block 1A12-PE binding (Fig. 3A). RMP1-14 and RMP1-30 mAbs did not block 1A12-PE binding, but increasing concentrations resulted in an ~50% increase in 1A12-PE fluorescence intensity (Fig. 3A). Such a result suggests cooperative antibody binding where structural changes at one site increase binding at a second site and have been observed to collaboratively enhance the activity of PECAM-1 mAbs.[18,19]

Binding of RMP1-14-PE was blocked by itself and by each of the other PD-1 mAbs with an avidity order of 1A12, RMP1-30, and RMP1-14 (Fig. 3B). RMP1-30 can fully block itself (Fig. 3C). RMP1-30-PE binding was reduced by ~27% by low concentrations of 1A12, and this level of blocking remained constant at higher concentrations of 1A12. RMP1-14 blocked RMP1-30 binding by ~25% at high concentrations of RMP1-14 (Fig. 3C).

These results support the use of RMP1-30 to stain for PD-1 in the presence of 1A12 or RMP1-14, such as in an immunotherapy experiment, but with an ~25% decrease in fluorescence intensity if the therapeutic mAb is bound to PD-1. The epitope blocking characteristics of mAbs from BioLegend and BioXcell were compared and found to be similar (Supplementary Fig. S2).

The heavy and light (kappa) chain signal and variable domain amino acid sequences of 9G2 and 1A12 are shown in Figure 3D and should be useful for further modeling immunotherapy and developing novel bispecifics. The sequence of RMP1-14 has been published.[20]

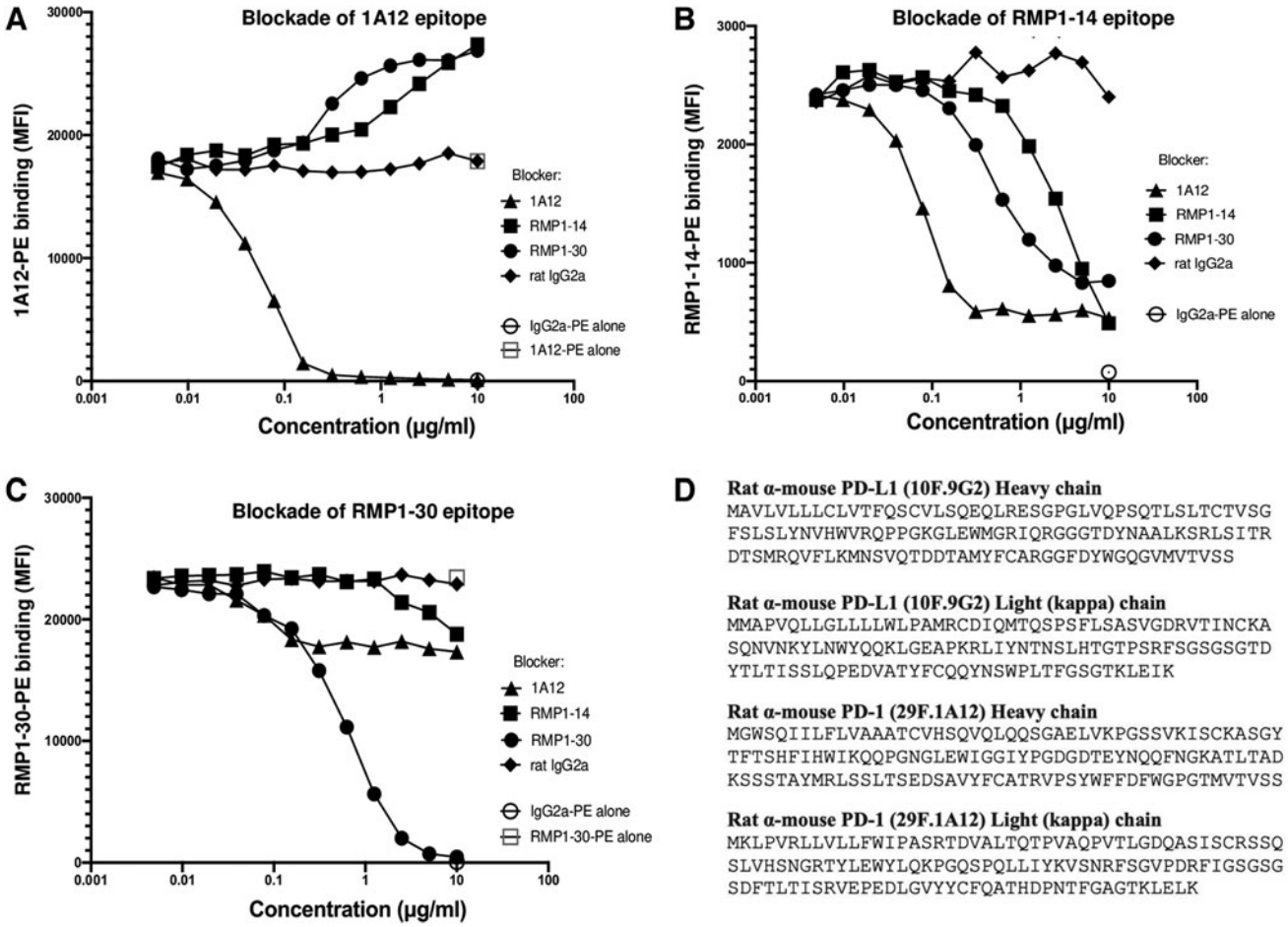

FIG. 3. Epitope blockade by PD-1 mAbs and antibody sequences. Flow cytometric analysis of **(A)** 1A12, RMP1-14, and RMP1-30 blockade of 1A12-PE binding. Replicates $n=5$. **(B)** 1A12, RMP1-14, and RMP1-30 blockade of RMP1-14-PE binding. Replicates $n=3$. **(C)** 1A12, RMP1-14, and RMP1-30 blockade of RMP1-30-PE binding. Replicates $n=5$. **(D)** Signal and variable domain amino acid sequences of PD-L1 mAb 9G2 and PD-1 mAb 1A12 heavy and kappa light chains.

Conclusions

In conclusion, 9G2, MIH6, and 1A12 can stain and block PD-L1 and PD-1, respectively, with subnanomolar affinity. RMP1-14 can stain PD-1 and block but with ~100-fold lower affinity. Since both 1A12 and RMP1-14 block and are rat IgG2a, they would be expected to have the same mechanism of action but different dose responses.[21,22] Since FDA-approved human PD-1 mAbs all have high affinity and blocking capacity,[23–28] mouse tumor immunotherapy experiments with 1A12 more closely model the human therapeutic mAbs.

Combination immunotherapy experiments with RMP1-14 may misestimate the potency of the second agent because of a less persistent blockade of PD-1. The human therapeutic antibodies are human IgG4 that has low effector function while both 1A12 and RMP1-14 are rat IgG2a that has moderate effector function. Even better modeling might be achieved using syngeneic effectorless Fc versions of 1A12.

Authors' Contributions

M.T.B contributed to conceptualization, investigation, writing—original draft, and writing—review and editing. L.Y. was involved in investigation and writing—review and editing. A.N.K. carried out investigation and writing—review and editing. G.J.F. took charge of conceptualization, resources, supervision, funding acquisition, investigation, writing—original draft, and writing—review and editing.

Author Disclosure Statement

G.J.F. has patents/pending royalties on the PD-1/PD-L1 pathway from Roche, Merck MSD, Bristol-Myers-Squibb, Merck KGA, Eli Lilly, Boehringer-Ingelheim, AstraZeneca, Dako, Leica, Mayo Clinic, and Novartis. G.J.F. has served on advisory boards for Roche, Bristol-Myers-Squibb, Xios, Origimed, Triursus, iTeos, NextPoint, IgM, Jubilant, Trillium, IOME, GV20, and Geode. G.J.F. has equity in Nextpoint, Triursus, Xios, iTeos, IgM, Trillium, Invaria, GV20, and Geode. M.T.B., L.Y., and A.N.K. have no disclosures to declare.

Funding Information

This study was supported by grants from the National Institutes of Health P01 AI56299 and P01 CA236749 to G.J.F.

Supplementary Material

Supplementary Figure S1
Supplementary Figure S2
Supplementary Figure S3

References

1. Agata Y, Kawasaki A, Nishimura H, Ishida Y, Tsubata T, Yagita H, and Honjo T: Expression of the PD-1 antigen on the surface of stimulated mouse T and B lymphocytes. Int Immunol 1996;8:765–772.
2. Dong H, Strome SE, Salomao DR, Tamura H, Hirano F, Flies DB, Roche PC, Lu J, Zhu G, Tamada K, Lennon VA, Celis E, and Chen L: Tumor-associated B7-H1 promotes T-cell apoptosis: A potential mechanism of immune evasion. Nat Med 2002;8:793–800.
3. Freeman GJ, Long AJ, Iwai Y, Bourque K, Chernova T, Nishimura H, Fitz LJ, Malenkovich N, Okazaki T, Byrne MC, Horton HF, Fouser L, Carter L, Ling V, Bowman MR, Carreno BM, Collins M, Wood CR, and Honjo T: Engagement of the PD-1 immunoinhibitory receptor by a novel B7 family member leads to negative regulation of lymphocyte activation. J Exp Med 2000;192:1027–1034.
4. Iwai Y, Ishida M, Tanaka Y, Okazaki T, Honjo T, and Minato N: Involvement of PD-L1 on tumor cells in the escape from host immune system and tumor immunotherapy by PD-L1 blockade. Proc Natl Acad Sci U S A 2002;99:12293–12297.
5. Juneja VR, McGuire KA, Manguso RT, LaFleur MW, Collins N, Haining WN, Freeman GJ, and Sharpe AH: PD-L1 on tumor cells is sufficient for immune evasion in immunogenic tumors and inhibits CD8 T cell cytotoxicity. J Exp Med 2017;214:895–904.
6. Eppihimer MJ, Gunn J, Freeman GJ, Greenfield EA, Chernova T, Erickson J, and Leonard JP: Expression and regulation of the PD-L1 immunoinhibitory molecule on microvascular endothelial cells. Microcirculation 2002;9:133–145.
7. Yamazaki T, Akiba H, Iwai H, Matsuda H, Aoki M, Tanno Y, Shin T, Tsuchiya H, Pardoll DM, Okumura K, Azuma M, and Yagita H: Expression of programmed death 1 ligands by murine T cells and APC. J Immunol 2002;169:5538–5545.
8. Kanai T, Totsuka T, Uraushihara K, Makita S, Nakamura T, Koganei K, Fukushima T, Akiba H, Yagita H, Okumura K, Machida U, Iwai H, Azuma M, Chen L, and Watanabe M: Blockade of B7-H1 suppresses the development of chronic intestinal inflammation. J Immunol 2003;171:4156–4163.
9. Liang SC, Latchman YE, Buhlmann JE, Tomczak MF, Horwitz BH, Freeman GJ, and Sharpe AH: Regulation of PD-1, PD-L1, and PD-L2 expression during normal and autoimmune responses. Eur J Immunol 2003;33:2706–2716.
10. Matsumoto K, Inoue H, Nakano T, Tsuda M, Yoshiura Y, Fukuyama S, Tsushima F, Hoshino T, Aizawa H, Akiba H, Pardoll D, Hara N, Yagita H, Azuma M, and Nakanishi Y: B7-DC regulates asthmatic response by an IFN-gamma-dependent mechanism. J Immunol 2004;172:2530–2541.
11. Pauken KE, Torchia JA, Chaudhri A, Sharpe AH, and Freeman GJ: Emerging concepts in PD-1 checkpoint biology. Semin Immunol 2021;52:101480.
12. Zou W, Wolchok JD, and Chen L: PD-L1 (B7-H1) and PD-1 pathway blockade for cancer therapy: Mechanisms, response biomarkers, and combinations. Sci Transl Med 2016;8:328rv4.
13. Topalian SL, Hodi FS, Brahmer JR, Gettinger SN, Smith DC, McDermott DF, Powderly JD, Carvajal RD, Sosman JA, Atkins MB, Leming PD, Spigel DR, Antonia SJ, Horn L, Drake CG, Pardoll DM, Chen L, Sharfman WH, Anders RA, Taube JM, McMiller TL, Xu H, Korman AJ, Jure-Kunkel M, Agrawal S, McDonald D, Kollia GD, Gupta A, Wigginton JM, and Sznol M: Safety, activity, and immune correlates of anti-PD-1 antibody in cancer. N Engl J Med 2012;366:2443–2454.
14. Rodig N, Ryan T, Allen JA, Pang H, Grabie N, Chernova T, Greenfield EA, Liang S, Sharpe AH, Lichtman AH, and Freeman GJ: Endothelial expression of PD-L1 and PD-L2 downregulates CD8+ T cell activation and cytolysis. Eur J Immunol 2003;33:3117–3126.
15. Barber DL, Wherry EJ, Masopust D, Zhu B, Allison JP, Sharpe AH, Freeman GJ, and Ahmed R: Restoring function in exhausted CD8 T cells during chronic viral infection. Nature 2006;439:682–687.
16. Latchman Y, Wood CR, Chernova T, Chaudhary D, Borde M, Chernova I, Iwai Y, Long AJ, Brown JA, Nunes R, Greenfield EA, Bourque K, Boussiotis VA, Carter LL, Carreno BM, Malenkovich N, Nishimura H, Okazaki T, Honjo T, Sharpe AH, and Freeman GJ: PD-L2 is a second ligand for PD-1 and inhibits T cell activation. Nat Immunol 2001;2:261–268.

17. Zhao M, Kiernan CH, Stairiker CJ, Hope JL, Leon LG, van Meurs M, Brouwers-Haspels I, Boers R, Boers J, Gribnau J, van IWFJ, Bindels EM, Hoogenboezem RM, Erkeland SJ, Mueller YM, and Katsikis PD: Rapid in vitro generation of bona fide exhausted CD8+ T cells is accompanied by Tcf7 promotor methylation. PLoS Pathog 2020;16:e1008555.
18. Chacko AM, Nayak M, Greineder CF, Delisser HM, and Muzykantov VR: Collaborative enhancement of antibody binding to distinct PECAM-1 epitopes modulates endothelial targeting. PLoS One 2012;7:e34958.
19. Roy RD, Rosenmund C, and Stefan MI: Cooperative binding mitigates the high-dose hook effect. BMC Syst Biol 2017;11:74.
20. Zhao P, Wang P, Dong S, Zhou Z, Cao Y, Yagita H, He X, Zheng SG, Fisher SJ, Fujinami RS, and Chen M: Depletion of PD-1-positive cells ameliorates autoimmune disease. Nat Biomed Eng 2019;3:292–305.
21. Arlauckas SP, Garris CS, Kohler RH, Kitaoka M, Cuccarese MF, Yang KS, Miller MA, Carlson JC, Freeman GJ, Anthony RM, Weissleder R, and Pittet MJ: In vivo imaging reveals a tumor-associated macrophage-mediated resistance pathway in anti-PD-1 therapy. Sci Transl Med 2017;9:eaal3604.
22. Dahan R, Sega E, Engelhardt J, Selby M, Korman AJ, and Ravetch JV: FcgammaRs Modulate the Anti-tumor Activity of Antibodies Targeting the PD-1/PD-L1 Axis. Cancer Cell 2015;28:285–295.
23. EMA. Assessment report Keytruda. International nonproprietary name: Pembrolizumab. London: European Medicines Agency; 2015. Available from: https://www.ema.europa.eu/en/documents/assessment-report/keytruda-epar-public-assessment-report_en.pdf (accessed March 28, 2022).
24. EMA. Assessment report Opdivo. International nonproprietary name: Nivolumab. London: European Medicines Agency; 2015. Available from: https://www.ema.europa.eu/en/documents/assessment-report/opdivo-epar-public-assessment-report_en.pdf
25. Fessas P, Lee H, Ikemizu S, and Janowitz T: A molecular and preclinical comparison of the PD-1-targeted T-cell checkpoint inhibitors nivolumab and pembrolizumab. Semin Oncol 2017;44:136–140.
26. Scapin G, Yang X, Prosise WW, McCoy M, Reichert P, Johnston JM, Kashi RS, and Strickland C: Structure of full-length human anti-PD1 therapeutic IgG4 antibody pembrolizumab. Nat Struct Mol Biol 2015;22:953–958.
27. Wang C, Thudium KB, Han M, Wang XT, Huang H, Feingersh D, Garcia C, Wu Y, Kuhne M, Srinivasan M, Singh S, Wong S, Garner N, Leblanc H, Bunch RT, Blanset D, Selby MJ, and Korman AJ: In vitro characterization of the anti-PD-1 antibody nivolumab, BMS-936558, and in vivo toxicology in non-human primates. Cancer Immunol Res 2014;2:846–856.
28. Zhang J, Dang F, Ren J, and Wei W: Biochemical aspects of PD-L1 regulation in cancer immunotherapy. Trends Biochem Sci 2018;43:1014–1032.

Address correspondence to:
Gordon J. Freeman
Department of Medical Oncology
Dana-Farber Cancer Institute
450 Brookline Avenue
Boston, MA 02115
USA

E-mail: gordon_freeman@dfci.harvard.edu

Received: December 26, 2021
Accepted: June 23, 2022

Monoclonal Antibody
10F.9G2
Against mouse PD-L1 (CD274, B7-H1)

Antigen Used for Immunization

Plasmid DNA expressing mouse PD-L1, boosted with CHO cells stably transfected with mouse PD-L1.

Method of Immunization

Female Lewis strain rats (Harlan Sprague–Dawley, Inc., Indianapolis, IN) were prepared for cDNA immunization by injecting 100 μL of 10 mM cardiotoxin (Sigma Chemical Company, St. Louis, MO) in 0.9% saline into the tibialis anterior muscle of each hind limb. Five days later, 100 μL of 1 mg/mL purified murine PD-L1 cDNA in the pAXEF mammalian expression vector in 0.9% saline was injected into each regenerating anterior tibialis anterior muscle of each rat. The cDNA immunization was repeated three times at 2- to 3-week intervals. Rats were then immunized with $1–5 \times 10^7$ CHO-mPD-L1 transfectants four times at 2- to 5-week intervals. Five days before fusion, the rat was immunized with both cDNA (200 μg) and cells (5×10^7).

Parental Cell Line Used for Fusion

Sp2/0

Selection and Cloning Procedure

Spleen cells were fused with Sp2/0 myeloma cells, cloned, and the hybridomas screened by enzyme-linked immunoassay (ELISA) for reactivity with a murine PD-L1 fusion protein (mPD-L1-mIgG2a), followed by cell surface staining of murine PD-L1–transfected 300.19 cells and COS cells and for lack of reactivity with untransfected cells and murine PD-L2–transfected cells.

Heavy and Light Chains of Immunoglobulin

Rat IgG2b, Kappa

Specificity

Screened by ELISA for reactivity with murine PD-L1-mIgG2a fusion protein, followed by cell surface staining of murine PD-L1–transfected 300.19 cells and COS cells and for lack of reactivity with untransfected cells and murine PD-L2–transfected cells. Recognizes an epitope in the extracellular domain of mouse PD-L1.

Specific Antigen Identified

Mouse PD-L1 (CD274, B7-H1)

Availability

	Yes	No
Tissue culture supernatant	[ ]	[x]
Ascitic fluid	[ ]	[x]
Hybridoma cells	[ ]	[x]

Hybridoma has been commercially licensed to many companies and is broadly available in purified and conjugated formats. Sequence provided in associated publication.

References

6. Eppihimer MJ, Gunn J, Freeman GJ, Greenfield EA, Chernova T, Erickson J, and Leonard JP: Expression and regulation of the PD-L1 immunoinhibitory molecule on microvascular endothelial cells. Microcirculation 2002;9: 133–145.
14. Rodig N, Ryan T, Allen JA, Pang H, Grabie N, Chernova T, Greenfield EA, Liang S, Sharpe AH, Lichtman AH, and Freeman GJ: Endothelial expression of PD-L1 and PD-L2 downregulates CD8+ T cell activation and cytolysis. Eur J Immunol 2003;33:3117–3126.

Address correspondence to:
Gordon Freeman
Department of Medical Oncology
Dana-Farber Cancer Institute
450 Brookline Avenue
Boston, MA 02215

E-mail: gordon_freeman@dfci.harvard.edu

Monoclonal Antibody 29F.1A12 Against mouse PD-1 (CD279)

Antigen Used for Immunization

Plasmid DNA expressing mouse PD-1, and murine PD-1-mIgG2a fusion protein

Method of Immunization

Female Lewis strain rats (Harlan Sprague–Dawley, Inc., Indianapolis, IN) were prepared for cDNA immunization by injecting 100 μL of 10 mM cardiotoxin (Sigma Chemical Company, St. Louis, MO) in 0.9% saline into the tibialis anterior muscle of each hind limb. Five days later, 100 μL of 1 mg/mL purified murine PD-1 cDNA in the pAXEF mammalian expression vector in 0.9% saline was injected into each regenerating anterior tibialis anterior muscle of each rat. The cDNA immunization was repeated three times at 2- to 3-week intervals. Rats were then immunized with murine PD-1-mIgG2a fusion protein four times at 2- to 5-week intervals. Five days before fusion, the rat was immunized with both cDNA (200 μg) and murine PD-1-mIgG2a fusion protein.

Parental Cell Line Used for Fusion

Sp2/0

Selection and Cloning Procedure

Spleen cells were fused with Sp2/0 myeloma cells, cloned, and the hybridomas screened by enzyme-linked immunoassay (ELISA) for reactivity with murine PD-1-mIgG2a fusion protein, developed with goat antirat kappa, followed by cell surface staining of murine PD-1–transfected 300.19 cells and COS cells and for lack of reactivity with untransfected cells.

Heavy and Light Chains of Immunoglobulin

Rat IgG2a, Kappa

Specificity

Specific for mouse PD-1 by ELISA for reactivity with murine PD-1-mIgG2a fusion protein developed with goat antirat kappa-HRP. Cell surface staining of murine PD-1–transfected 300.19 cells and COS cells and for lack of reactivity with untransfected cells. Recognizes an epitope in the extracellular domain of mouse PD-1.

Specific Antigen Identified

Mouse PD-1 (CD279)

Availability

	Yes	No
Tissue culture supernatant	[ ]	[x]
Ascitic fluid	[ ]	[x]
Hybridoma cells	[ ]	[x]

Hybridoma has been commercially licensed to many companies and is broadly available in purified and conjugated formats. Sequence provided in associated publication.

References

9. Liang SC, Latchman YE, Buhlmann JE, Tomczak MF, Horwitz BH, Freeman GJ, and Sharpe AH: Regulation of PD-1, PD-L1, and PD-L2 expression during normal and autoimmune responses. Eur J Immunol 2003; 33:2706–2716.
15. Barber DL, Wherry EJ, Masopust D, Zhu B, Allison JP, Sharpe AH, Freeman GJ, and Ahmed R: Restoring function in exhausted CD8 T cells during chronic viral infection. Nature 2006; 439:682–687.

Address correspondence to:
Gordon Freeman
Department of Medical Oncology
Dana-Farber Cancer Institute
450 Brookline Avenue
Boston, MA 02215

E-mail: gordon_freeman@dfci.harvard.edu